TRANSIENT THERMAL-HYDRAULICS CONSIDERATIONS OF TANDEM MIRROR Li–Pb COOLED BLANKETS DURING START-UP/SHUTDOWN OPERATIONS

Kaveh TAGHAVI and Nasr M. GHONIEM

Fusion Engineering and Physics Group, School of Engineering and Applied Science, University of California, Los Angeles, Los Angeles, CA 90024, USA

Received 13 January 1984

The operational aspects of fusion reactors are being recognized as important ingredients of the design process. In this paper, we present analyses and modeling relevant to the understanding of blanket performance during transients. The use of Li–Pb as a blanket coolant is considered in this paper from the viewpoint of transient operation during initial start-up. When Li–Pb is first introduced into the blanket tubes in the form of a molten metal, freezing/blockage and thermal shock to the tubes may occur. We first model the transient thermal behavior of the coolant (Li–Pb)-tube system. We then proceed to analyze the thermal shock to the blanket tubes upon contact with the hot Li–Pb. It is shown that freezing/blockage due to excessive heat losses from the Li–Pb coolant is not a major design consideration. However, thermal stresses caused by differential expansion during transients should be mitigated by appropriate pre-heating of blanket modules.

1. Introduction

Recently, two major design studies [1,2] for Tandem Mirror Reactors have considered the use of the molten metal Li–Pb as a tritium breeder and cooling medium. Both the WITAMIR-I [1] and Mirror Advanced Reactor Study (MARS) [2] have successfully demonstrated the viability of the $Li_{17}Pb_{83}$ eutectic LiPb as a coolant/breeder material. LiPb is compatible with both austenitic and ferritic alloys. The combination of LiPb and the ferritic alloy HT-9 shows successful performance in a high temperature blanket, up to about 480 °C. Magnetic fields in Tandem Mirror Reactors are not so high as to result in excessive MHD pressure losses. Since LiPb must be kept always molten during reactor operation, it is important to understand how this will be achieved. In this paper, we analyze the engineering problems that result during the initial start-up phases of a specific Li–Pb cooled blanket. Since such analysis is expected to be design dependent, we focus here on the MARS blanket [2]. In section 2, we first model possible freezing/blockage of blanket tubes during initial flooding with LiPb. This is then followed by analysis of thermal shock to the blanket tubes, upon contact with hot LiPb. The necessary requirement of pre-heating of the primary system and blanket modules are finally presented.

2. Freezing/blockage during initial start-up

Fig. 1 shows the cross-section of the mirror advanced reactor study (MARS) blanket. The blanket consists of two arrays of tubes and one array of beams. Cold coolant (350 °C) enters the blanket from the top, passes

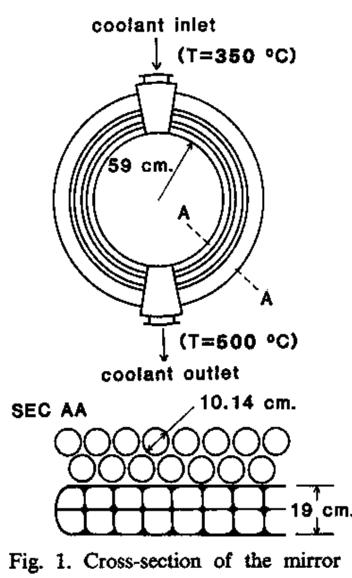

Fig. 1. Cross-section of the mirror advanced reactor study (MARS) blanket.

through the tubes and beams while being heated up, and finally hot coolant (500 °C) leaves the blanket from the bottom.

In this section possible freezing of the hot LiPb during initial flooding of relatively colder tubes of the blanket is considered. It is desired to determine conditions leading to freezing of the coolant or bloackage of the tube during initial flooding.

2.1. Modeling

Consider a vertical tube representing one of the circular MARS tubes at room temperature being flooded from the bottom with hot liquid LiPb. Such a model is shown in fig. 2. Upon initial contact of the cold tube wall and hot coolant, the temperature of the interface between the tube and the hot liquid reaches a unique temperature calculated as [3]

$$\frac{T_c - T_w}{T_l - T_c} = \left(\frac{\rho_l c_{pl} k_l}{\rho_w c_{pw} k_w} \right)^{1/2}, \tag{1}$$

where T_c is the contact temperature and subscripts w and l are related to tube wall and liquid coolant, respectively. The interface stays at this temperature only for a short period of time. Thereafter, the interface temperature will be dictated by the balance of the heat going into and out of the interface.

In cases where the contact temperature is below the coolant temperature, a thin frozen layer may form inside the tube. The rate of growth or shrinkage of this layer is then dependent upon the magnitude of the heat

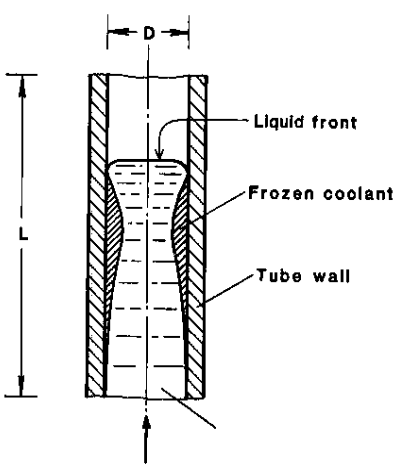

Fig. 2. Model for flooding of HT-9 tube with hot LiPb.

fluxes in and out of the film. The frozen film is heated by the adjacent flow of hot coolant while it loses heat to the cold tube wall. For a short period of time the magnitude of the heat transfer to the tube wall is higher than that received from the hot coolant which results in growth of the frozen film. Thereafter, the tube temperature will rise and the heat lost to the tube wall will decrease. The heat gained from the hot coolant, however, will remain almost constant. At some point the frozen film starts remelting. To analyze this problem, two separate models describing the phenomena in short times and relatively longer times will be considered. The two models are matched by studying the transient response of the tube wall to a sudden surface temperature increase.

2.1.1. Model for short times

For short times, most of the heat lost to the tube wall goes to raise the tube temperature. Therefore, it may be appropriate to approximate the tube wall with a semi-infinite slab. Fig. 3 shows such a model. Assuming that no significant temperature drop occurs across the frozen layer, an energy balance may be written to obtain a relation for the growth of the frozen layer.

$$\rho_s H_{sf} \frac{d\delta_s}{dt} = q_w'' - q_l'', \tag{2}$$

where

$$q_w'' = k_w (T_m - T_e)/(\pi \alpha_w t)^{1/2}, \tag{3}$$

$$q_l'' = h_l (T_l - T_m). \tag{4}$$

Substituting eqs. (3) and (4) into eq. (2), and integrating, we obtain the following relation for δ_s:

$$\delta_s = \frac{2 k_w (T_m - T_e)}{\rho_s H_{sf} \sqrt{\pi \alpha_w}} t^{1/2} - \frac{h_l (T_l - T_m)}{\rho_s H_{sf}} t. \tag{5}$$

It is evident from eq. (5) that the frozen layer thickness is zero at $t = 0$ and starts to grow as $t^{1/2}$ for small t. At some time, t_{max}, the frozen layer thickness reaches a maximum and decreases with time thereafter. The

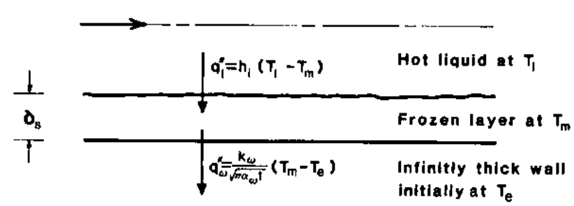

Fig. 3. Physical model describing the freezing for short periods of time.

parameters t_{max} and $\delta_{s,max}$ may be calculated as

$$t_{max} = \frac{k_w^2 (T_m - T_e)^2}{\pi \alpha_w h_l^2 (T_l - T_m)^2}, \quad (6)$$

$$\delta_{s,max} = \frac{k_w^2 (T_m - T_e)^2}{\pi \alpha_w \rho_s H_{sf} h_l (T_l - T_m)}. \quad (7)$$

The layer thickness will eventually become zero at $t = 4t_{max}$ when the present model will no longer be applicable.

2.1.2. Model for long times

For long times, almost all the heat transferred to the tube wall is in turn lost to the environment. It is assumed that a linear temperature profile exists in the frozen film and the tube wall. Fig. 4 shows such a model. An energy balance at the frozen layer-hot liquid interface yields:

$$\rho_s H_{sf} \frac{d\delta_s}{dt} = q''_w - q''_l, \quad (8)$$

where

$$q''_w = (T_m - T_e)/(\delta_w/k_w + 1/h_e), \quad (9)$$

and

$$q''_l = h_l(T_l - T_m). \quad (10)$$

Eqs. (8), (9), and (10) may be combined to obtain

$$\frac{d\delta_s}{dt} = (T_m - T_e)/(\delta_w/k_w + 1/h_e) - h_l(T_l - T_m)/(\rho_s H_{sf}). \quad (11)$$

In order to integrate eq. (11), information is needed as to when the infinite tube thickness model breaks down and the present model utilizing steady state temperature profile is applicable. The time for matching the two models is obtained by studying the transient response of a finite slab to a sudden jump in its surface temperature.

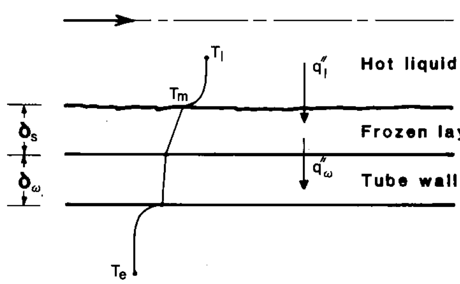

Fig. 4. Physical model describing the freezing for long periods of time.

2.2. LiPb-HT-9 case

In this section the preceeding analysis is applied to the specific case of a cold ($T_{w,init} = T_e = 20\,°C$) HT-9 tube flooded with hot ($T_l = 350\,°C$) LiPb. Table 1 lists the thermophysical properties of HT-9 and LiPb. The tube is about 10 cm I.D., 0.25 cm thick and 2 m long. The heat transfer coefficients inside and outside the tube (h_l and h_e) are calculated by employing appropriate correlations for flow of liquid metals inside tubes and natural convetion on vertical surfaces, respectively. For the present case, the heat transfer coefficient inside the tube $h_l = 725$ W/m²K and outside the tube $h_e = 13$ W/m²K.

The contact temperature for this system is calculated from eq. (1) to be

$$T_c = 128\,°C. \quad (12)$$

This temperature is below the freezing temperature ($T_m = 235\,°C$) which suggests that some freezing may occur initially. Before attempting to obtain the frozen layer thickness as a function of time, the cut-off time between the two models for short and long time behavior must be evaluated. Fig. 5 shows the transient response of a 0.25 cm thick slab of HT-9 initially at 20 °C to a surface temperature of 235 °C. The plot is for the average temperature of the tube wall as a function of time. It is seen that at about 2 s the average temperature has almost reached its asymptotic value. At this point the results obtained for the frozen layer thickness (eqs. (5) and (11)) may be plotted for the LiPb-HT-9 case. Fig. 6 shows the dependence of the frozen layer thickness on

Table 1
Thermophysical properties of HT-9 and LiPb

Property	Unit	HT-9	LiPb
Melting temperature	°C	–	235 [d]
Density	kg/m³	7818 [b]	9350 [d]
Specific heat	J/kg K	460 [b]	159 [a]
Thermal conductivity	W/mK	29 [c]	16.6 [a]
Heat of fusion	J/Kg	–	2.47×10^4 [a]

[a] Estimated based on thermophysical properties of Li and Pb.
[b] Estimated based on thermophysical properties of similar materials.
[c] Ref. [1].
[d] Ref. [4].

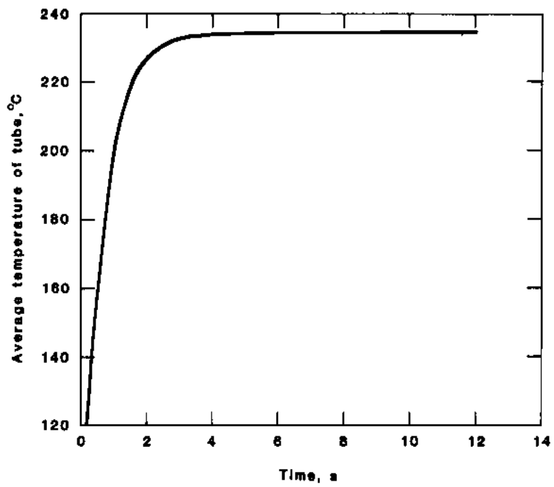

Fig. 5. Transient response of HT-9 tube to a surface temperature jump ($T_s = 235\,^\circ$C).

time. The film thickness increases with time for short times (solid line). However, at some point ($t = 2.2$ s), the short time model is not applicable and the long time model is used (dashed line). Thereafter, the film thickness decreases with time and becomes zero at $t = 13.3$ s. It is seen that the frozen film thickness reaches a maximum of 1.5 cm at $t = 2.2$ s which results in 28% blockage of the MARS blanket tubes. The freezing and remelting, however, lasts about 13.3 s. It is interesting to note that the frozen film obtained from the infinitely thick tube model (solid line) also demonstrates a similar behavior of growth and shrinkage (freezing and remelting).

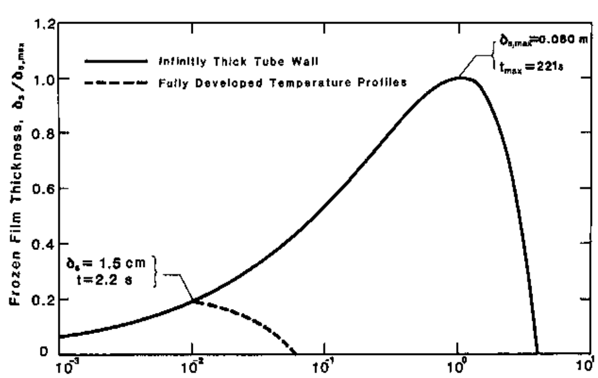

Fig. 6. Frozen layer thickness as a function of time.

2.3. Temperature variation of the coolant

In the model used for analysis, the coolant temperature was assumed to be constant. However, in the actual situation the coolant loses heat as it flows through the tube. We estimate here the coolant temperature drop along the tube.

Assuming that the coolant loses heat to the frozen film at $T_m = 235\,^\circ$C, the coolant temperature along the tube may be written as:

$$(T_{1,\text{out}} - T_m)/(T_{1,\text{in}} - T_m) = e^{-(4h_1L)/(\rho_1 D V_1 c_{p1})}, \quad (13)$$

where L and D are length and inner diameter of the tube and V_1 is the coolant velocity. For a coolant velocity of 2 m/s, the coolant exit temperature is calculated as:

$$T_{1,\text{out}} = 347.8\,^\circ\text{C} \quad \text{or} \quad T_{1,\text{in}} - T_{1,\text{out}} = 2.2\,^\circ\text{C}. \quad (14)$$

It may be concluded that the coolant temperature drop is negligible and that the coolant temperature is reasonably constant.

3. Thermal shock during initial start-up

During initial flooding of the blanket tubes the relatively cold tube material is suddenly exposed to hot LiPb. This results in thermal shock across the tube wall. In this section the thermal shock of the tube material upon initial flooding with hot LiPb is investigated.

3.1. Modeling

The largest thermal shock is predicted to occur at the tube entrance where an initially cold tube is suddenly exposed to hot coolant from inside. Transient thermal strain distributions through the tube wall are obtained numerically by solving the time-dependent heat conduction equation. Fig. 7 shows such a model. The thermal stress history of the tube wall is subsequently determined with the use of plate theory. The instantaneous strain at various tube wall locations are given by:

$$\epsilon = \alpha_{\text{th}}(\overline{T} - T(x)), \quad (15)$$

where

$$\overline{T} = \frac{1}{\delta_w}\int_0^{\delta_w} T(x)\,dx, \quad (16)$$

where α_{th} is the coefficient of thermal expansion of the tube material, δ_w is the tube wall thickness, and $\overline{T}$ is the average wall temperature.

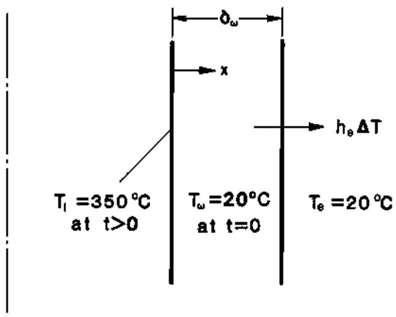

Fig. 7. Physical model for thermal shock during initial flooding.

3.2. LiPb-HT-9 case

Fig. 8 shows the results of sample calculations for HT-9 where the thermal strain is plotted as a function of time for various locations across the tube wall. It is shown that on the coolant side of the tube, the compressive strain exceeds the yield strength of the material for short periods of time. This leads to plastic deformation and strain ratcheting over several cycles. Fig. 9 shows similar results for a thicker tube ($\delta = 7$ mm), which corresponds to the manifolds. The maximum strain (compression and tensile) is seen to have not been affected by the tube thickness. The characteristic time, however, is much longer for the thicker tube. Fig. 9 also includes the strain related to the yield stress. The inside of the tube experiences strain larger than the yield limit for a couple of seconds. Fresh start-up is not likely to be a frequent event, however, considering problems associated with fatigue, radiation embrittlement, and uncertainties in HT-9 data, any stress in excess of the yield stress should be avoided. Therefore, it is concluded that the blanket needs to be pre-heated to a temperature higher than the ambient (20 °C). Similar results have

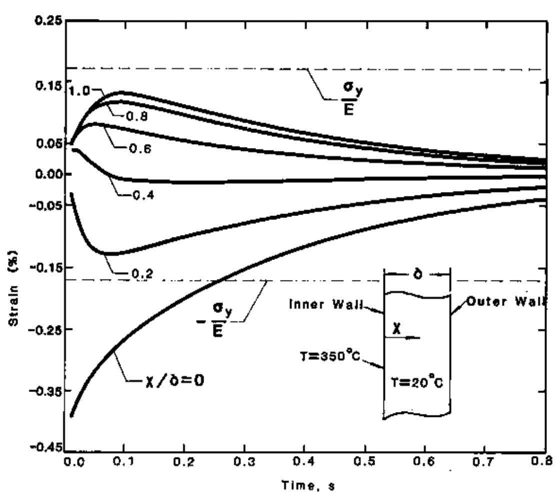

Fig. 8. Transient thermal strain versus time for HT-9 ($\delta = 2.5$ mm).

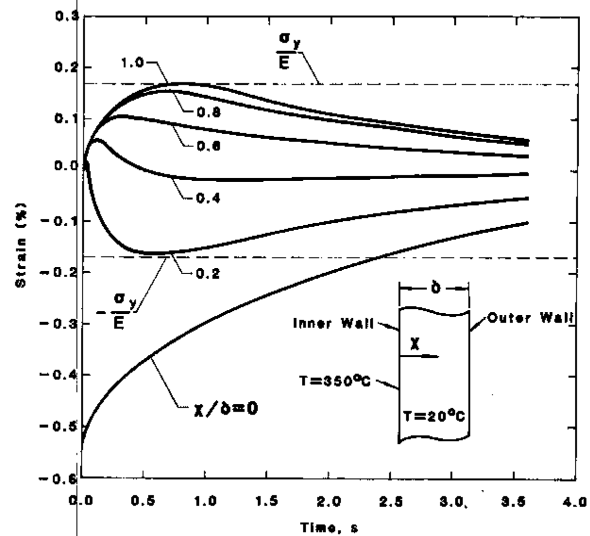

Fig. 9. Transient thermal strain versus time for HT-9 ($\delta = 7$ mm).

Table 2
Peak strain results for different initial conditions

T_{initial} [°C]	$\epsilon_{\text{peak}}/(1-\nu)\epsilon_y$
20	2.99
100	2.26
200	1.35
300	0.452
350	0

The yield strain, ϵ_y, for HT-9 is taken to be $\sigma_y/E = 0.0017$ [7].

Table 3
Comparison of maximum strain for stainless steel 316, 2.25 Cr-1 Mo, and HT-9 for a tube initially at 20 °C exposed to coolant at 350 °C

	SS-316	2.25 Cr-1 Mo	HT-9
σ_{design} [a] at 400 °C [GPa]	0.227 [5]	0.185 [6]	0.194 [7]
ν at 400 °C	0.294 [8]	0.283 [6]	0.265 [8]
E at 400 °C [GPa]	167 [8]	183 [6]	175 [8]
$E\epsilon_{\max}/(1-\nu)\sigma_{\text{design}}$	1.73	1.68	1.17

[a] Based on ASME boiler and pressure vessel code.

been obtained for flooding with hot LiPb of tubes with different initial temperatures. Table 2 shows the ratio of the peak strain (at the inner surface and at time = 0) to the yield strain for different pre-heating temperatures. From the standpoint of fatigue failure, however, it is desirable to lower this ratio as much as possible.

Strain results have also been obtained for tubes of similar size and made of HT-9, stainless steel, and $2\frac{1}{4}$Cr–1 Mo. The results indicate that HT-9 suffers the smallest maximum strain. Table 3 is a summary the results. In a companion paper [9], various possible options will be considered regarding pre-heating requirements of blanket tubes.

4. Summary and conclusions

Thermal hydraulics of the LiPb cooled blanket during start-up and shutdown transients has been considered in this paper. It has been shown that during flooding of cold blanket tubes with hot LiPb, some freezing of LiPb may temporarily occur before it remelts again. The degree of freezing has been found not to cause any significant blockage. The thermal shock caused by flooding, however, has been found to exceed the yield stress if the blanket is initially kept at room temperature. This indicates that some pre-heating of the blanket is necessary to avoid severe thermal shock and eventual thermal fatigue. Calculations for various degrees of pre-heating have shown that blanket modules must be pre-heated to within about 50 °C of the LiPb inlet temperature during operation, in order to avoid thermal fatigue.

Nomenclature

c_{pl} specific heat of the liquid coolant,
c_{pw} specific heat of the tube wall,
D inside diameter of the tube,
E modulus of elasticity,
H_{sf} latent heat of fusion,
h_e heat transfer coefficient outside tube,
h_l heat transfer coefficient inside tube,
k conductivity of the liquid coolant,
k_w conductivity of the tube wall,
L tube length,
q_l'' liquid side heat flux,
q_w'' tube wall heat flux,
T_c contact temperature,
T_e environment temperature,
T_l liquid coolant temperature,
T_m coolant freezing temperature,
$\bar{T}$ average temperature of the tube wall,
t time,
V_l liquid coolant velocity,
α_{th} coefficient of the thermal expansion of the tube wall,
α_w thermal diffusivity of tube wall,
ν Poisson's ratio,
δ_s frozen layer thickness,
δ_w tube wall thickness,
ϵ strain,
ϵ_y yield strain,
σ stress,
ρ_s frozen layer density.

Acknowledgements

The authors would like to acknowledge the stimulating discussions with the Engineering groups of the START study at UCLA, and the MARS study at LLL. In particular, they wish to thank Professor R.W. Conn, Dr. M.Z. Youssef, and Mr. S.P. Grotz for their involvement. The financial support of the Department of Energy through contract # DE-AM03-76SF00034/P.A. DE-AT03-80ER52061 with UCLA is greatly acknowledged.

References

[1] B. Badger et al., WITAMIR-I, a tandem mirror reactor study (1980).
[2] B.G. Logan et al., Mirror Advanced Reactor Study (MARS), Nucl. Technol./Fusion 4 (1983) 563.
[3] E.R.G. Eckert and R.M. Drake, Analysis of Heat and Mass Transfer (McGraw Hill, New York, 1972).
[4] N.J. Hoffman, A. Darnell and J.A. Blink, Properties of lead–lithium solutions, 4th ANS Topical Meeting on the Technology of Controlled Nuclear Fusion, King of Prussia, PA, 14–17 Oct. 1980.
[5] M.A. Abdou et al., Blanket comparison and selection study, Argonne National Laboratory, Report ANL/FPP/83-1 (Oct. 1983).
[6] Design Data, Vol. 1, Nuclear Systems Materials Handbook, Hanford Engineering Development Laboratory, TID-26666 (1977).
[7] R. Amodeo and N.M. Ghoniem, Constitutive design equations for thermal creep deformation of HT-9, J. Nucl. Mater. 122 & 123 (1984) 91.
[8] J.M. Rawlz et al., Assessment of martensitic steels in magnetic fusion devices, General Atomic Co., Report GA-A15749 (1980).
[9] K. Taghavi and N.M. Ghoniem, Primary loop conditioning and design constraints of Li–Pb cooled tandem mirror reactors during start-up/shutdown operations, Nucl. Engrg. Des./Fusion 1 (1984) 375, this issue.